

Article

Current Conditions and Projected Changes in Crop Water Demand, Irrigation Requirement, and Water Availability over West Africa

Imoleayo Ezekiel Gbode^{1,*}, Gulilat Tefera Diro², Joseph Daniel Intsiful³ and Jimy Dudhia⁴¹ Department of Meteorology and Climate Science, Federal University of Technology, Akure 340252, Nigeria² Canadian Network for Regional Climate and Weather Processes, Centre Pour l'Étude et la Simulation du Climat à l'Échelle Régionale, University of Quebec at Montreal, 201 President-Kennedy Avenue, Montreal, QC H2X 3Y7, Canada; gulilatfef@gmail.com³ Division of Mitigation and Adaptation, Green Climate Fund, Incheon 22004, Korea; jintiful@gcfund.org⁴ Microscale and Mesoscale Meteorology Laboratory, National Center for Atmospheric Research, Boulder, CO 80305, USA; dudhia@ucar.edu

* Correspondence: iegbode@futa.edu.ng

Abstract: Climate variability and change greatly affect agricultural and water resource management over West Africa. This paper presents the current characteristics and projected change in regional crop water demand (CWD), irrigation requirement (IR), and water availability (WA) over West Africa. Observed and simulated daily rainfall, minimum temperature, maximum temperature, and evapotranspiration are used to derive the above agro-meteorological and hydrological variables. For future periods, high-resolution climate data from three regional climate models under two different scenarios, i.e., representative concentration pathway (RCP) 4.5 and 8.5, are considered. Evaluation of the characteristics of present-day CWD, IR, and WA indicated that the ensemble mean of the model-derived outputs reproduced the prevailing spatial patterns of CWD and IR. Moreover, the wetter part of the domain, especially along the southern coast, was correctly delineated from the drier northern regions, despite having biases. The ensemble model also simulated the annual cycle of water supply and the bimodal pattern of the water demand curves correctly. In terms of future projections, the outcomes from the study suggest an average increase in the CWD by up to 0.808 mm/day and IR by 1.244 mm/day towards the end of the twenty-first century, compared to the baseline period. The hot-spot areas, where there is higher projected increment in CWD and IR, are over Senegal, Southern Mali, and Western Burkina Faso. In most cases, WA is projected to decrease towards the end of the twenty-first century by -0.418 mm/day. The largest decline in WA is found to be over Guinea and most of the eastern parts of West Africa. Despite the current under-utilization of the existing groundwater resources, the threat of global warming in reducing future WA and increasing CWD suggested caution on the scale of irrigation schemes and management strategies. The outcomes from the study could be a crucial input for the agricultural and water managers for introducing effective measures to ensure sustainability of irrigated farm lands.

Keywords: irrigation requirement; crop water demand; water availability; West Africa; climate change; regional climate models



Citation: Gbode, I.E.; Diro, G.T.; Intsiful, J.D.; Dudhia, J. Current Conditions and Projected Changes in Crop Water Demand, Irrigation Requirement, and Water Availability over West Africa. *Atmosphere* **2022**, *13*, 1155. <https://doi.org/10.3390/atmos13071155>

Academic Editor: Gianni Bellocchi

Received: 1 May 2022

Accepted: 11 July 2022

Published: 21 July 2022

Publisher's Note: MDPI stays neutral with regard to jurisdictional claims in published maps and institutional affiliations.



Copyright: © 2022 by the authors. Licensee MDPI, Basel, Switzerland. This article is an open access article distributed under the terms and conditions of the Creative Commons Attribution (CC BY) license (<https://creativecommons.org/licenses/by/4.0/>).

1. Introduction

Agriculture is a critical sector for the economy of most countries in West Africa. It contributes, on average, 23% and 35% to the gross domestic product (GDP) of sub-Saharan and West Africa [1,2], respectively. Furthermore, about 60% and 65% of the population are directly or indirectly engaged in a wide range of agricultural activities [1,2] in the corresponding regions. The population of West African countries is growing by 2.75% per year, with major cities growing at the rate of 9% per year [3]. This implies that countries will require more food production to feed the increased population.

While crop production is the main sector of agriculture, water shortage is the main limiting factor for crop production [4]. This is because water resources are acute and exhibit strong spatio-temporal variation, as rainfall is only received during the monsoon months and the land is dry during the rest of the year. Irrigation has been important to obtain maximum agricultural yield and to supplement the rainfed system. It is natural to expect irrigated agriculture to expand to feed the increasing population. Increases in greenhouse gases (GHG) may alter factors that determine the atmospheric water demand, precipitation, temperature and, hence, crop water requirement, thereby affecting water planning and evaluation. Irrigation water needs are highly sensitive to changes in precipitation, temperature, and carbon dioxide levels. Therefore, any change in water availability and irrigation water requirements will have a profound effect on agricultural productivity.

Although scientific findings from climate change research have improved our understanding of the relationship between global warming and crop water demand, there are yet huge uncertainties as to when climate will change and how these changes will affect the supply and demand of water in the future, which is crucial for water resource planners and farmers. For instance, higher evapotranspiration due to temperature rise suggests a higher amount of water for irrigation. Higher temperature, on the other hand, will change the crop physiology and shorten the crop growing period, which in turn will reduce the irrigation days. This implies that these two competing factors determine the total irrigation water demand in a future warmer world. Owing to this uncertainty and other reasons, including the agricultural scale and planting structure suitable for water resources of a given area, numerous studies have been conducted to investigate the impact of climate change on irrigation demand, both at the regional and global scale [5–11]. However, a comprehensive assessment of the present-day characteristics of crop water demand (CWD), irrigation requirements (IR), and water availability (WA) in terms of their climatology, inter- and intra-annual variability, as well as a thorough projected assessment for a future warmer climate from an ensemble of higher spatial resolution regional climate models is yet to be carried out for West Africa.

The aim of this study is to assess the current characteristics and the projected changes in crop water demand, irrigation requirement, and water availability over West Africa using observations, reanalysis data, and regional climate models (RCMs) developed as part of the Coordinated Regional Climate Downscaling Experiment (CORDEX, [12]). For the future projection, two emission scenarios were considered. The reliable estimates of CWD, IR, and WA over the region would help greatly in the rational utilization of available water resources for irrigation and management practices.

This paper is organized as follows: after this introduction, data and methods employed in the analysis are described in Section 2. Section 3 presents results and discussion, which include an assessment of how realistically the RCMs simulate key characteristics during current climate conditions. This section also provides a detailed analysis of how water availability, crop water demand, and irrigation requirement will change in future under the two emission scenarios. Finally, summary and conclusion are provided in Section 4.

2. Data, Models and Methods

2.1. Data and Models

The climate variables used in this assessment are high-resolution daily precipitation, daily minimum temperature, daily maximum temperature, and evapotranspiration dataset from various sources. Below is the description of the observational and reanalysis datasets:

The precipitation data considered are those in the Climate Hazards Group InfraRed Precipitation with Stations (CHIRPS, [13]) daily dataset. CHIRPS uses TIR imagery and gauge data in addition to monthly precipitation climatology, CHPCLim, and atmospheric model rainfall fields from the NOAA Climate Forecast System, version 2 (CFSv2). Despite the satellite imageries in CHIRPS being available at higher resolution (0.05°), it is interpolated to 0.25° resolution to match the resolution of the fifth generation of the European Centre for Medium Range Weather Forecasts (ECMWF) reanalysis (ERA5). Daily evapo-

transpiration as well as daily maximum and minimum temperature fields are obtained from ERA5 reanalysis. ERA5 reanalysis is produced by combining the Integrated Forecast System with data assimilation at a spatial resolution of 0.25° grid and at hourly time intervals [14].

Three regional climate models (RCMs) participating in the Coordinated Regional Climate Downscaling Experiment (CORDEX, [12]) framework was retrieved from the Earth System Grid Federation (ESGF) portal [15]. These RCMs included models from the Swedish Meteorological and Hydrological Institute, Rossby Centre (SMHI, [16]), the Climate Limited-area Modelling Community (CCLM, [17]), and the Helmholtz-Zentrum Geesthacht, Climate Service Center, Max Planck Institute for Meteorology (REMO, [18]). Common to these regional climate models are the Max Planck's Earth Systems Model [19] low-resolution runs that were used as initial and boundary conditions to force the regional model simulations.

2.2. Methods

The model data obtained for assessment are in daily frequency running from 1976 to 2100. Four analysis periods are chosen: the reference or historical period (1976–2005) and three future periods representing near future (2011–2040), mid-future (2041–2070), and far future (2071–2100). For future climate, two RCPs (RCP4.5 and RCP 8.5) were considered [20].

2.2.1. Derivation of Irrigation Water Requirements and Other Hydrometeorological Variables

Using the above climatological data, the CWD, IR, and WA are derived using FAO-recommended approaches and simple hydrological balance equations at the grid point level. It must be noted that this approximation for WA does not consider later inflow of water from the neighboring grid point.

Here, CWD will be represented by crop reference evapotranspiration (ET_o), which is considered as a proxy for the water requirement under a well-watered condition. Although there are a number of methods available for the estimation of ET_o , in this study, Baier–Robertson [21] and Hargreave [22] methods are employed, due to their simplicity and the accuracy of estimates as recommended in the FAO paper 56 [23]. The formulation of each method is given below:

Hargreaves and Samani (hereafter HETo) [22]:

$$ET_o = 0.0023(T_{\text{mean}} + 17.8)(T_{\text{max}} - T_{\text{min}})^{0.5} R_a$$

Baier–Robertson (hereafter BRETto) [21]:

$$ET_o = 0.157T_{\text{max}} + 0.158(T_{\text{max}} - T_{\text{min}}) + 0.109R_a - 5.39$$

where T_{mean} , T_{max} , T_{min} , and R_a are the mean, maximum, minimum temperatures, and extraterrestrial radiation, respectively.

Even if this reference value is not crop specific, it can be parameterized by a correction factor (crop coefficient, K_c) for each crop type. This correction factor is found to range between 0.8 and 1 for most crops growing over West Africa [10]; therefore, using the crop water demand computed using this method can be justified.

The irrigation water need or irrigation requirement (IWN or IR), which is the amount of water required to sustain a crop, is also derived using the ET_o and effective rainfall (Pe), i.e., $IR = ET_o - Pe$.

Various approaches are proposed to estimate effective precipitation (Pe). For instance, Doll [5] uses two empirical functions of actual precipitation with a threshold value of 8.3 mm/day. Others follow a look-up table estimated using an empirical method [24]. In this assessment, it is represented by the actual evapotranspiration (ET) [10]. Here, the actual evapotranspiration was computed from latent heat flux using latent heat of vaporization of water.

For WA, the terrestrial water storage is considered as a proxy of the water available for crop growth. The WA is computed as the difference between actual rainfall and actual evapotranspiration, i.e., $WA = PR - ET$.

These hydrological variables are estimated from observational datasets and from regional climate model outputs for present-day as well as for three future time horizons with two representative concentration pathways (RCPs: RCP 4.5 and 8.5). For the climate change assessment, the length of each time horizon is set to 30 years long, as recommended by WMO's guide to climatological practices [25].

2.2.2. Trend Analysis of Hydrological Variables

The first aspect of climate assessment is to evaluate the degree of accuracy of the CORDEX model-derived hydrological variables in representing the observed characteristics during the historical period. One of these characteristics is the presence of trends in WA, IR, and CWD. The Mann–Kendall trend test [26–28] is computed for areal averages to identify temporal trends. The second aspect of the analysis is to relatively compute the baseline scenario, for identifying the risk and exposure to the projected change in each of the three major climatic zones in West Africa: Guinea coast (4–8° N); Savannah (8–11° N); and Sahel (11–16° N), defined based on land use/land cover, climate, and ecosystem characteristics [29–32].

2.2.3. Projected Changes in Exposure under Enhanced GHGs

Providing future climate projections of the intensity and exposure of water stress indicators is certainly vital for effective adaptation to climate hazards. While projections will be developed using RCP 8.5 and 4.5, emphasis will be given to RCP 8.5 (higher emissions), because it is representative of the path the global community is currently on. Furthermore, by planning for higher emissions, it will be less likely to underestimate the impacts of climate change (and create a lack of preparedness). A comparison of results from the two scenarios will also be performed, as RCP 4.5 represents emission reductions. This can help people understand the impact of reducing emissions. In addition, analysis on changes in WA and IR will be carried out for the selected climatic zones.

3. Results and Discussion

3.1. Validation of CWD, IR and WA Characteristics in Current Climate

3.1.1. Spatial Variability

The spatial pattern of the annual climatology of CWD, IR, and WA based on observational and ensemble mean climate mode outputs is shown in Figure 1. Climatological observation-based results reveal lower values of available surface water and higher values of CWD and IR over the northern arid regions (e.g., from north of latitude 10° N). Conversely, relatively abundant surface water and low CWD and lower IR are noted over the southern part of the domain, especially along the southern coastline, as these regions are reflected by higher rainfall and lower ET_0 . The regional climate model simulation-derived crop water and irrigation demand reproduced the observed spatial pattern, although it shows slight underestimation of CWD and IR over central parts of the region along latitude 15° N, and overestimation over Senegal. The highest bias (0.58 mm/day) in WA is noted over the Guinea coast, whereas the largest bias in IR is noted over Sahel (−0.33 mm/day), as shown in Table 1. It is interesting to note that the temporal correlation between BRETo and HETo is greater than >0.95 (Figure S1, in the supplementary document), demonstrating their close resemblance, despite the fact that the BRETo method produced lower values of CWD and IR compared to the HETo counterpart, as reflected in the respective biases (Figure S2). This implies that, according to the BRETo estimation of CWD, irrigation activity could be practiced over a larger area. It has to be noted that the magnitude of CWD and IR simulation is more sensitive to the formulation of reference evaporation compared to the biases in temperature and radiation simulation.

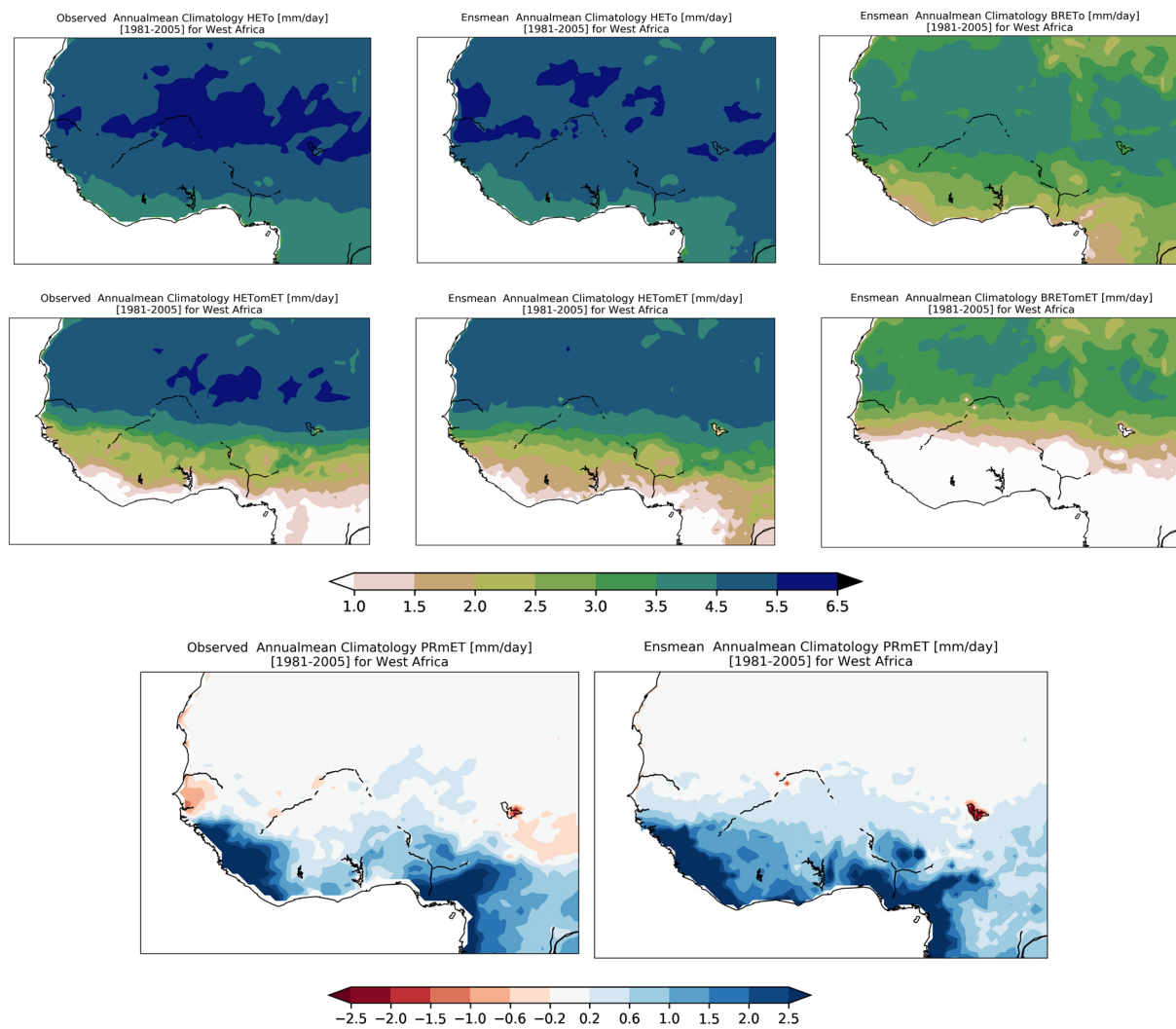


Figure 1. Annual mean climatology of crop water demand (**top row**), irrigation requirement (**middle row**) (mm/day) from observations/reanalysis data (**left**), and ensemble mean regional climate model output computed using HETo (**middle**) and BRETo (**right**) methods. Bottom panel is for water availability computed based on observational and reanalysis data (**left**) and from ensemble mean regional climate model outputs (**right**).

Table 1. Bias (model–observation) in irrigation requirement and water availability (mm/day/year) averaged over the three climatic zones—Guinea Coast, Savannah, and Sahel.

Bias	HETo-ET (Irrig. Requirement)	PR-ET (Water Availability)
Guinea Coast	−0.06	0.58
Savannah	−0.24	0.33
Sahel	−0.33	0.25

The figure also indicated that the ensemble mean generally reproduced the observed spatial pattern of annual climatology of water availability by delineating the wet regions of the southern domain accurately. However, the ensemble mean simulation overestimates the amount of WA of the region and misses the water deficit regions of Western Senegal but captures the deficit over Lake Chad. The overestimation of WA by the models mean simulation is mainly due to the overestimation of precipitation (not shown), although the evaporation is also slightly overestimated.

3.1.2. Temporal Variability

Present-day monthly distributions of CWD, IR, and WA for the selected three regions are shown in Figure 2. In Sahel and Savannah, the WA curve shows a monomodal pattern, peaking in August following the arrival of the intertropical convergence zone over the region but bimodal pattern in Guinea Coast. The observed bimodal pattern in Guinea Coast is not well represented in the model. The model captured the monomodal pattern very well, despite its overestimation of the peak. CWD and IR undergo a similar migration of annual cycles, with higher values during late winter/spring months, then decline and attain lower values during the monsoon season before rising again. The simulated annual cycle of CWD and IR also follows a similar pattern, suggesting that the models performed well in this regard. It is also noted that, while both CWD and IR follow a similar annual cycle, both in observation and models, the annual cycle of IR shows a strong contrast between summer/early autumn and the rest of the year, suggesting that it is sensitive to precipitation.

3.2. Projected Changes

Spatial Pattern of the Projected Changes

Figures 3 and 4 show the ensemble mean projected changes in CWD and IR, respectively, computed using HETo and the BRETo methods for future periods compared to the present day for RCP 8.5 (RCP 4.5) scenarios. In both methods, projected CWD and IR exhibit the largest increase under RCP 8.5 and for the far-future period. In the medium term, the average annual CWD and IR are expected to increase by 0.6 mm, with no notable differences between the RCP 4.5 and RCP 8.5 projections (Figures 3, 4, S3 and S4). The increase in annual CWD and IR is projected to continue in the latter part of the 21st century. It is also noted that RCP 8.5 prompts higher irrigation requirements than RCP 4.5. This substantial difference between RCP 4.5 and RCP 8.5 suggests that mitigation of the rise in GHG has an impact on the future irrigation water needs. The increased demand and the greater impact of the RCP 8.5 scenario found in this study are consistent with results from previous studies conducted for different locations [33].

The projected changes in WA revealed a decline over Guinea and most of the eastern parts of West Africa, especially over Nigeria, southern Republic of Benin, and Togo (Figures 5 and S5). The decline in WA is stronger but not statistically significant for the end of the century and for RCP 8.5 scenarios. WA is also projected to significantly increase over parts of Guinea, Sierra Leone, Liberia, southern Côte d'Ivoire and southern Ghana, especially for mid-future and RCP 8.5 scenarios.

The comparison of the projected changes across the individual models (not shown) also suggested that the increase in IR is consistent across the three models and with the ensemble mean, as all the three models agree in the sign of the change, though CCLM shows a stronger response, while SMHI-RCA shows the least sensitivity to climate change (not shown). Similarly, the comparison of the projected change in WA also suggested that the three models agree on the decline in WA by the end of the century, though the signal is not consistent in the recent future. The disagreement among models in the near-future projection is expected, as model uncertainty and internal climate variability are the key sources of uncertainty in the near-future projection, whereas scenario uncertainty dominates for the end of century projection [34].

It is also noted that future precipitation and evapotranspiration changes are primarily negative over most of the domain, particularly in Sahel, as shown in Figures 6 and 7. The decline is intensified and becomes statistically significant in the mid- and far-future periods. These results are consistent with past studies, which indicated that climate projections for West Africa are progressively warmer and drier [35,36]. Under these climate scenarios, future IR are projected to increase in both future periods.

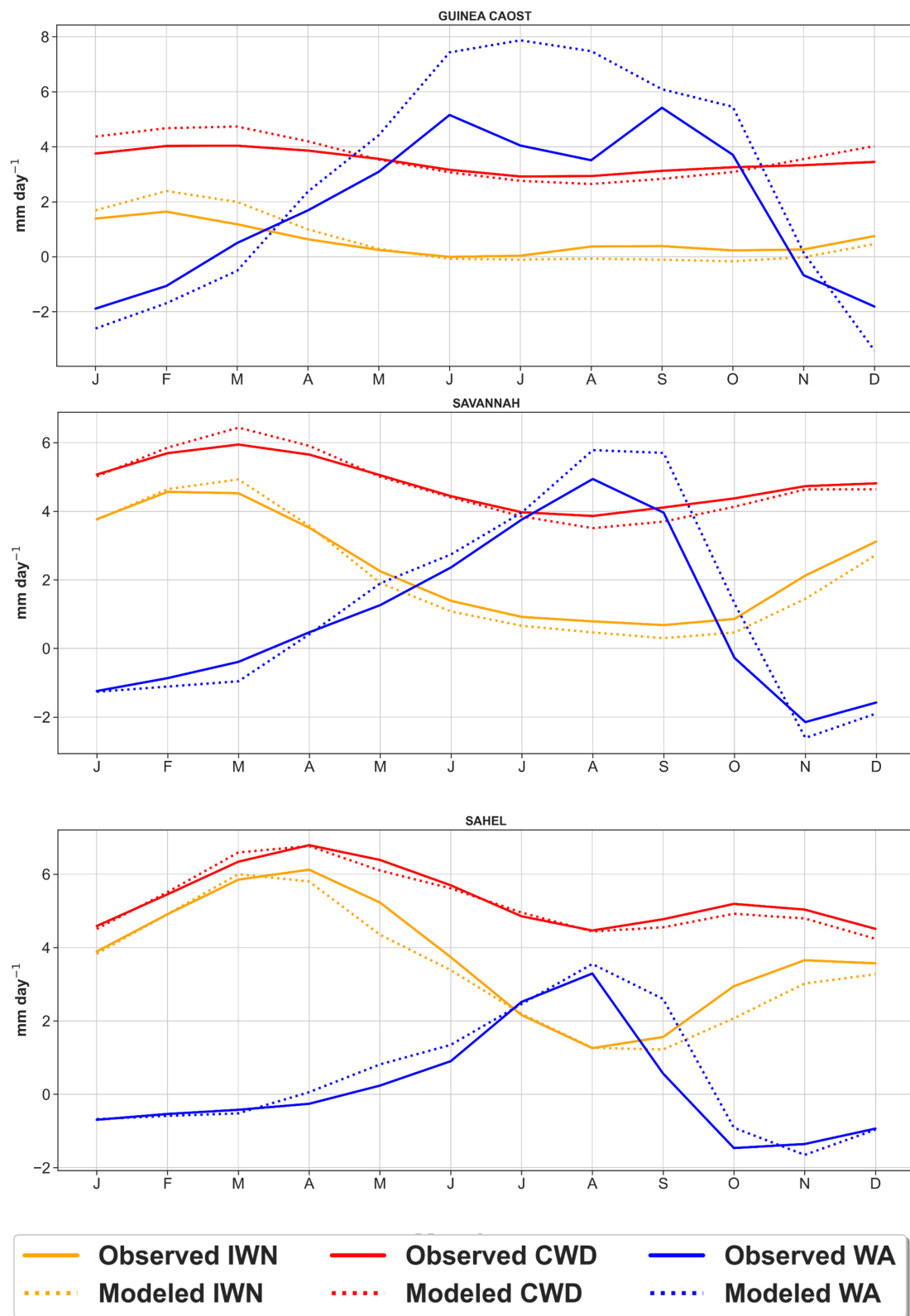


Figure 2. Annual cycle of daily mean CWD, IR, and WA (mm/day) for selected three sub-regions for the period 1981–2005. The continuous lines are meteorological observation-derived values, while the dotted lines represent estimation from the ensemble mean model simulations. HETo estimates are used for CWD and IWN/IR.

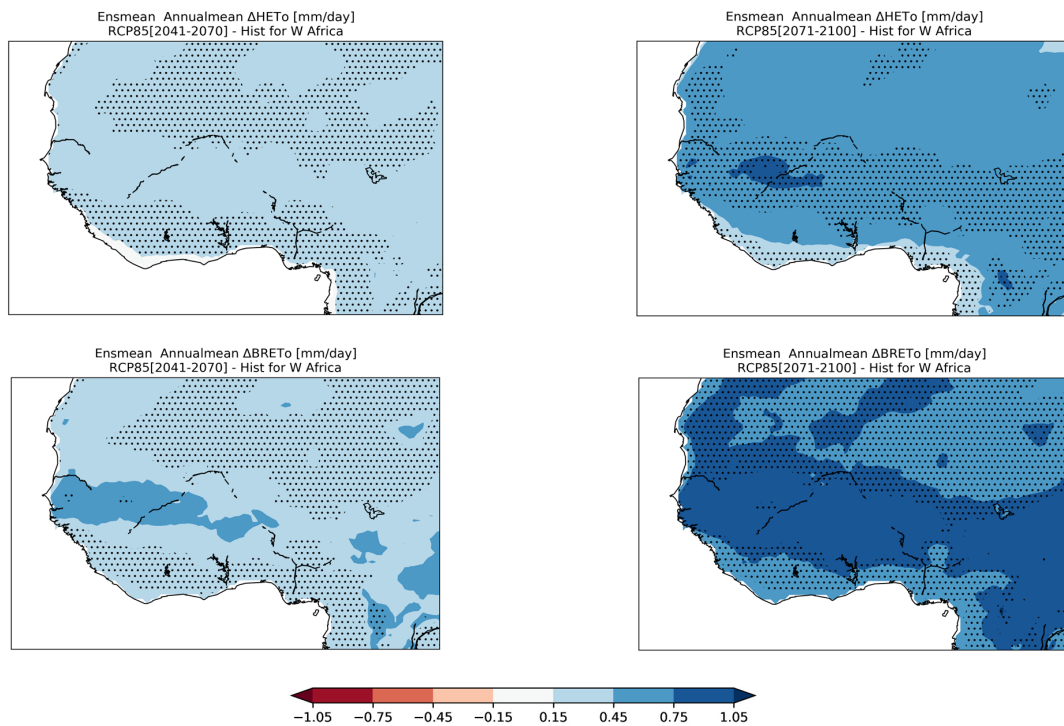


Figure 3. Projected changes in crop water demand (mm/day) for mid-future (**left** column) and far future (**right** column) computed using HETo (**top** panel) and BRETo (**bottom** panel) methods from the ensemble mean of regional climate models derived under RCP 8.5.

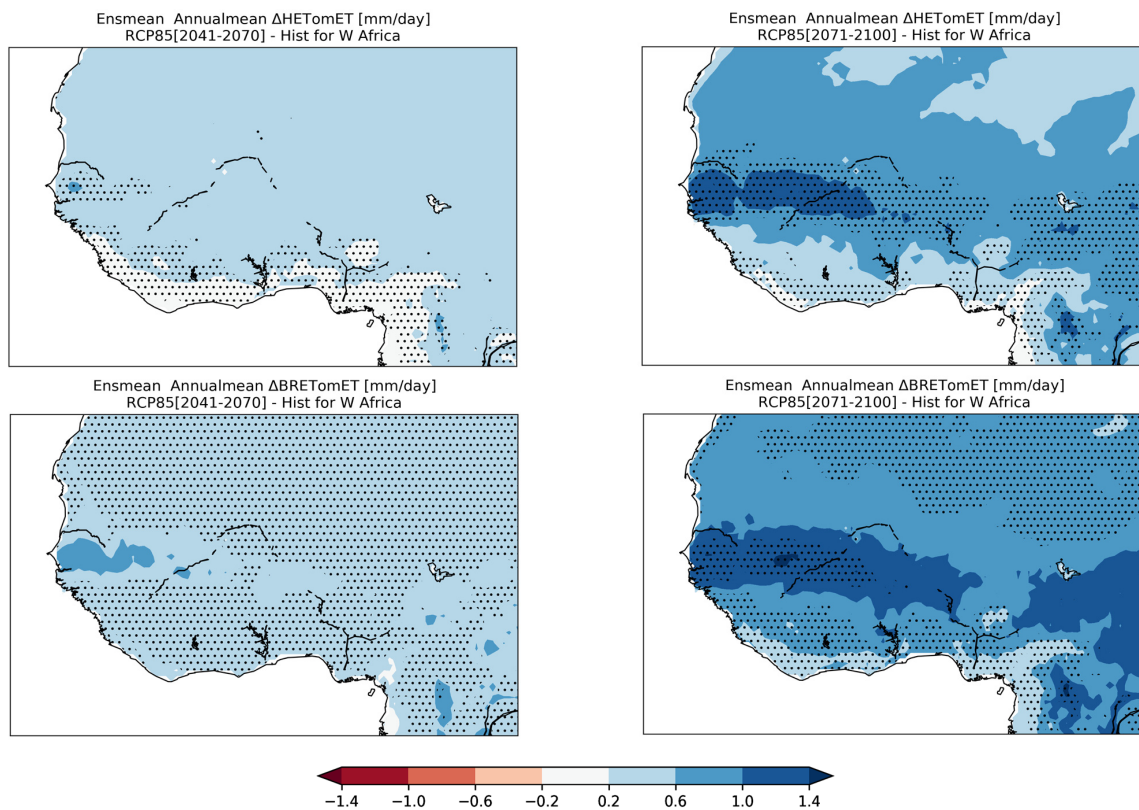


Figure 4. Projected changes in irrigation requirement (mm/day) computed using HETo (**top** row) and BRETo (**bottom** row) methods for mid-future (**left** column) and far future (**right** column) from the ensemble mean of regional climate models derived under RCP 8.5.

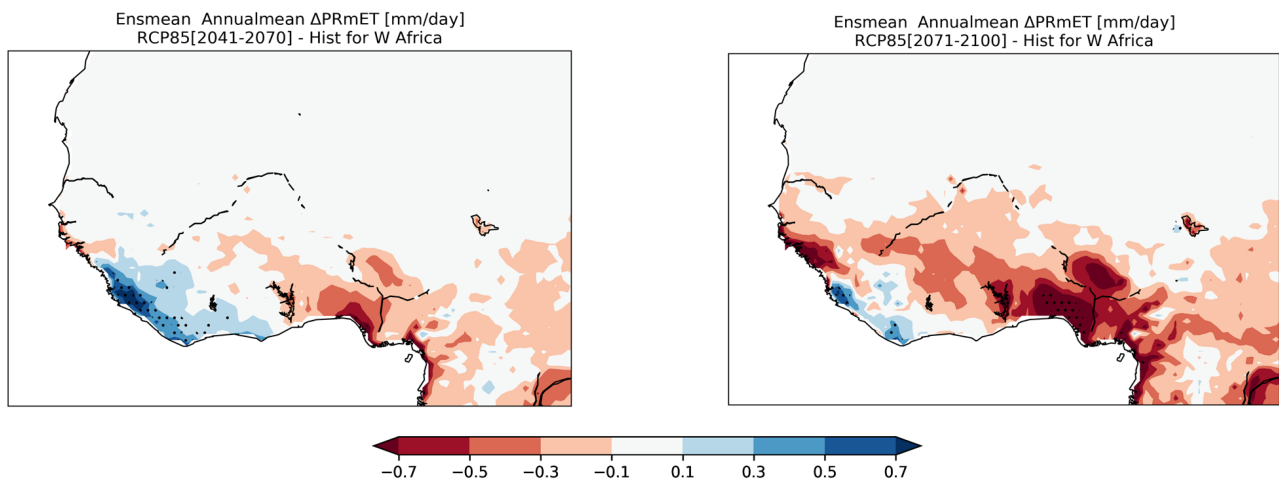


Figure 5. Projected changes in water availability (mm/day) for mid-future (**left** column) and far future (**right** column) from the ensemble mean of regional climate models derived under RCP 8.5.

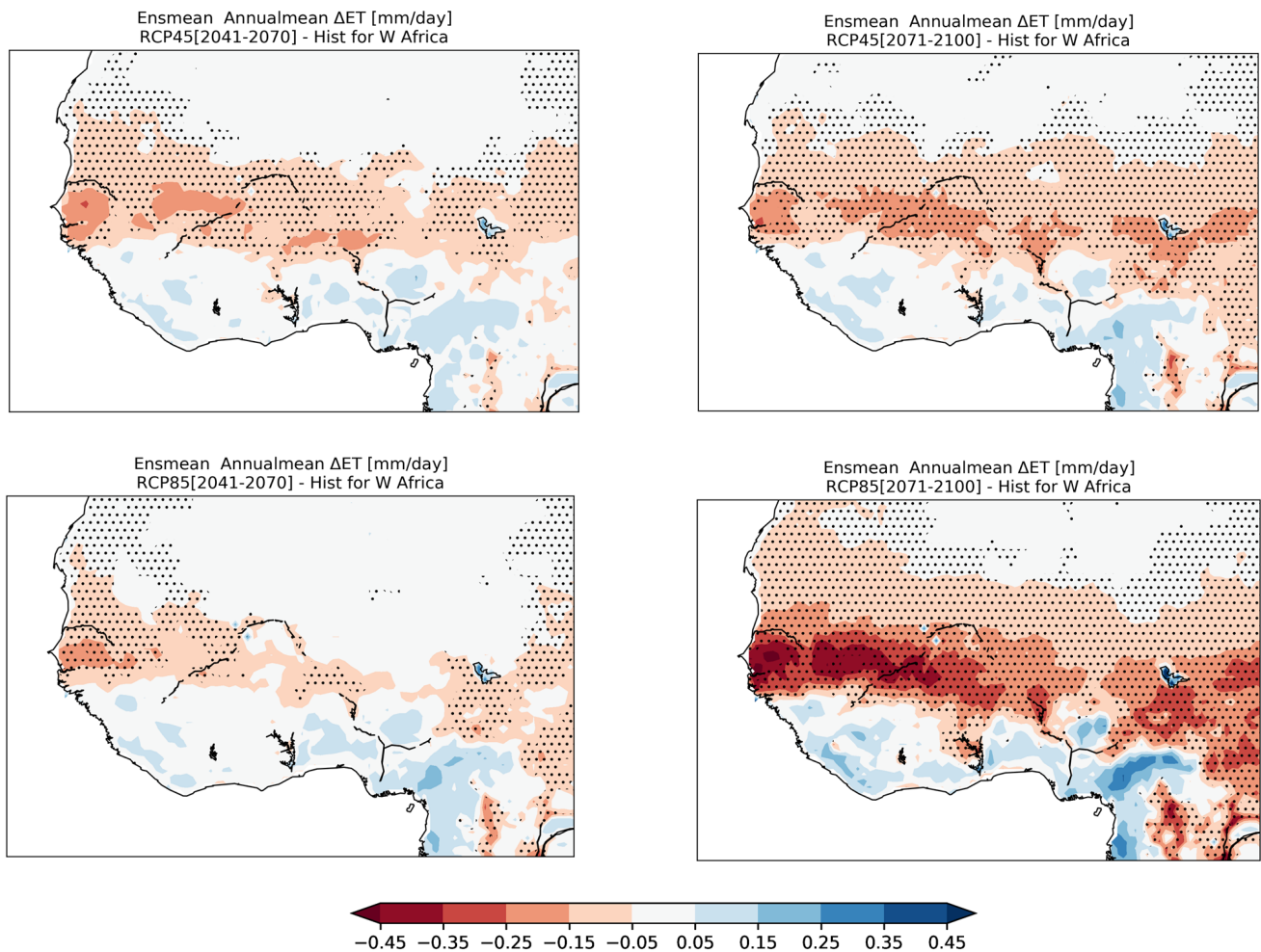


Figure 6. Projected changes in evapotranspiration (mm/day) for mid-future (**left** column) and far future (**right** column) from RCP4.5 (**top** row) and RCP8.5 (**bottom** row) scenarios. Regions with dots overlaid on the filled contour represent statistically significant at 0.05 level.

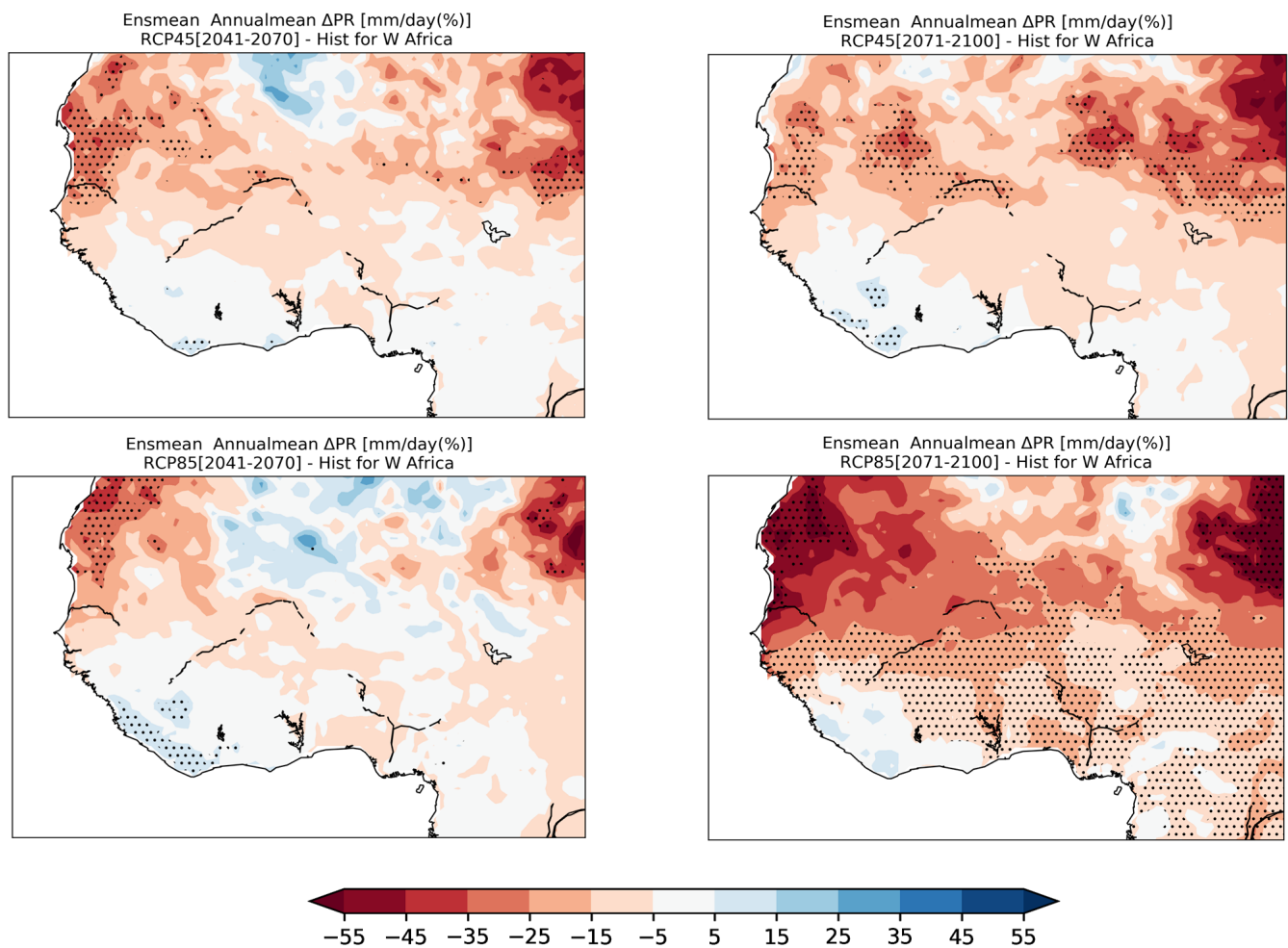


Figure 7. Projected changes in precipitation (%) for mid-future (**left** column) and far future (**right** column) from RCP4.5 (**top** row) and RCP8.5 (**bottom** row) scenarios. Regions with dots overlaid on the filled contour represent statistically significant at 0.05 level.

Figures 8–10 show a time series of the historical and future CWD, IR, and WA averaged over the three climatic zones - Guinea Coast, Savannah, and Sahel. It is clear that CWD and IR increase with time, especially in Guinea Coast and Savannah (Figure 8). The rate of increment in CWD increases significantly with latitude from 0.006 mm/day/year in Guinea Coast to 0.019 mm/day/year in Sahel in the future time for the RCP8.5 scenario, particularly towards the end of the century. Although there are increasing trends under RCP4.5, a significant increment occurred during the middle of the 21st century (Table 2). Trends in historical IR are positive in all the climatic zones, with a significant increase in the Guinea Coast (Figure 9). Similar to the CWD, statistically significant increasing trends are projected in all climatic zones under RCP 8.5. Under RCP 4.5, the trends also increased significantly in Guinea Coast and Savannah during the mid-21st century. Figure 10 shows a decrease in WA for Savannah and Sahel. This trend is expected to continue up to the mid-21st century in these zones, before becoming positive at the end of the century with the RCP 4.5 scenario. In Guinea Coast, the trends are negative in the last two climate epochs. A similar signal is expected in Savannah and Sahel with RCP8.5, although the decrease is not statistically significant (Table 2).

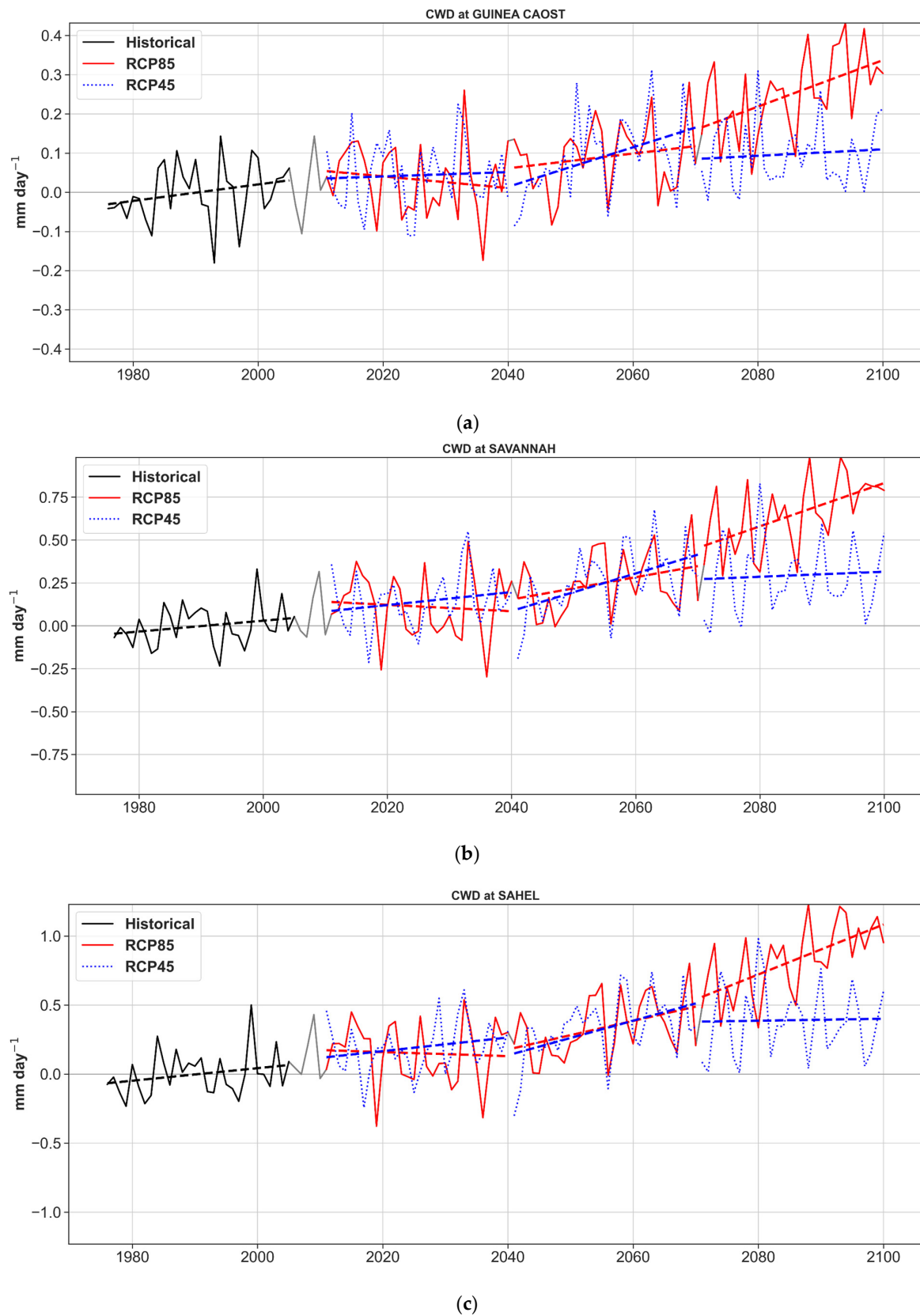


Figure 8. Historical and projected time series of annual mean daily CWD (mm/day) at (a) Guinea Coast, (b) Savannah, and (c) Sahel. The black line represents the historical period, while blue and red lines represent predicted values under RCP 4.5 and RCP 8.5 emission scenarios, respectively. The plotted values are departure from the baseline (1976–2005).

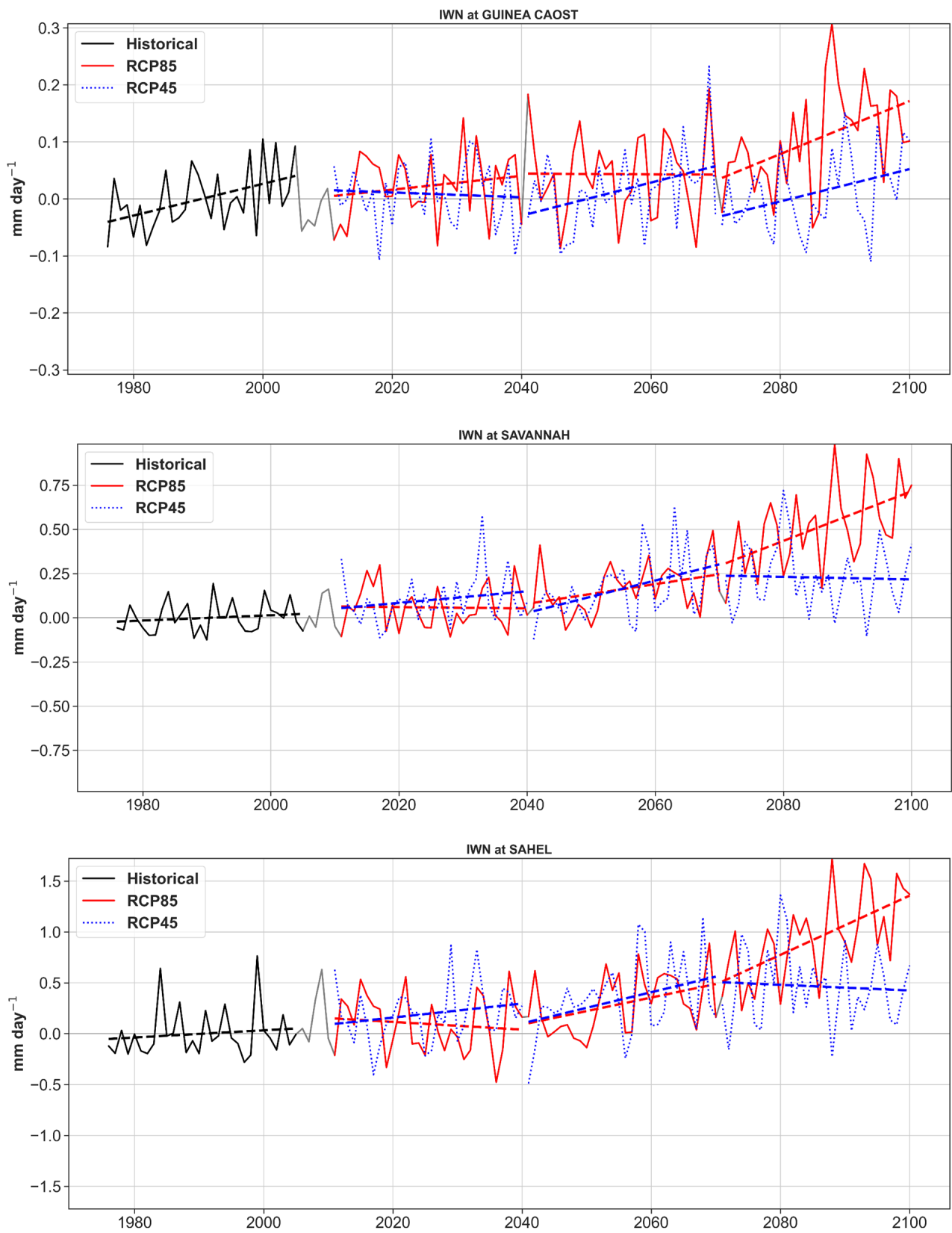


Figure 9. Same as Figure 8, but for IR.

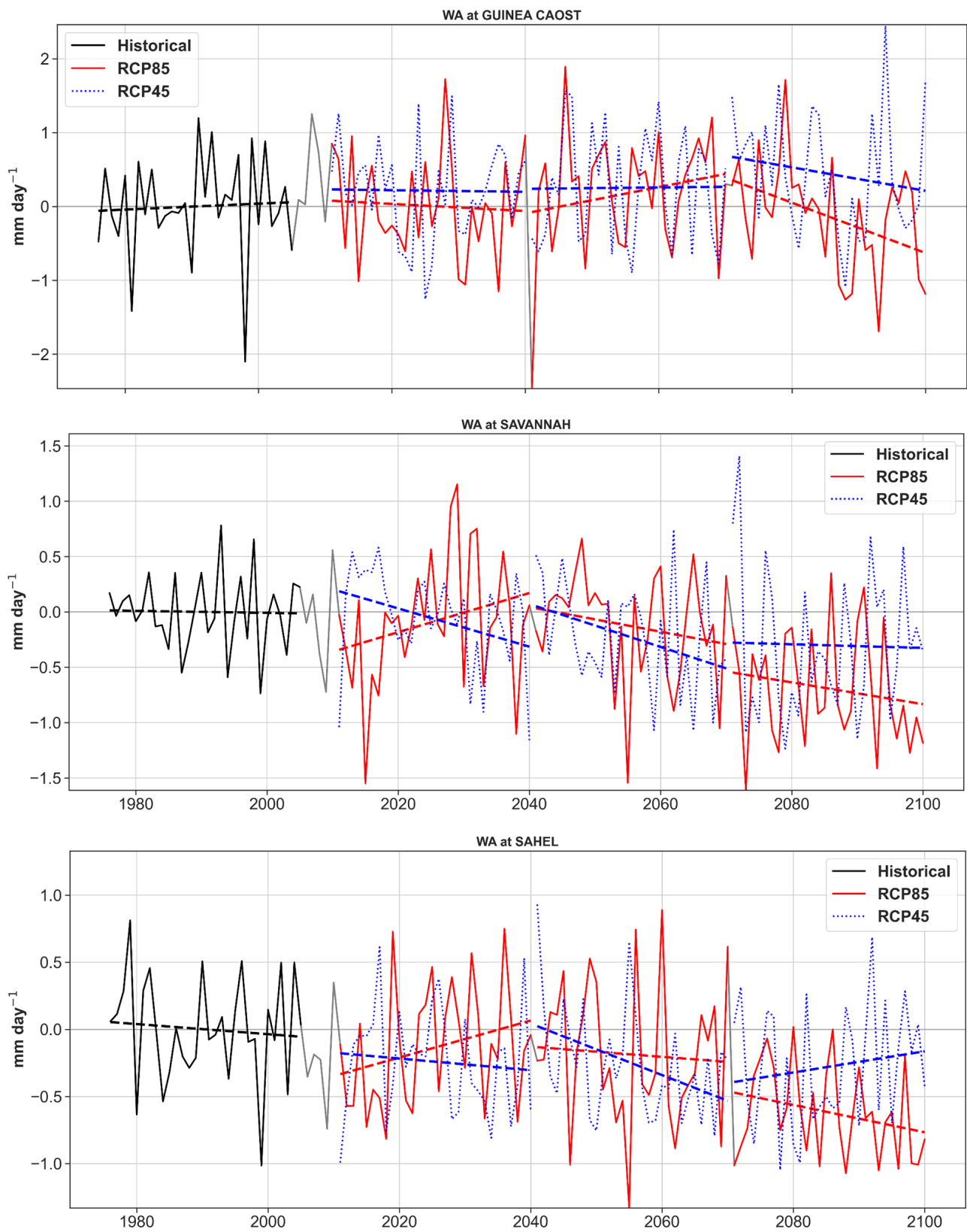


Figure 10. Same as Figure 8, but for WA.

Table 2. Summary of historical and projected trends in CWD, IR, and WA (mm/day/year) averaged over the three climatic zones; Guinea Coast, Savannah, and Sahel. Bold values depict significant trends at 0.05 level.

Episode	Period	Guinea Coast			Savannah			Sahel		
		CWD	IR	WA	CWD	IR	WA	CWD	IR	WA
Historical	1976–2005	0.002	0.003	0.009	0.002	0.001	−0.003	0.003	0.002	−0.001
	2011–2040	0.000	−0.001	0.001	0.003	0.003	−0.019	0.005	0.006	−0.007
RCP4.5	2041–2070	0.006	0.002	−0.002	0.010	0.009	−0.024	0.010	0.013	−0.015
	2071–2100	0.001	0.003	−0.025	0.002	0.001	0.012	0.001	−0.003	0.008
RCP8.5	2011–2040	−0.002	0.001	−0.006	−0.003	−0.001	0.016	−0.002	−0.006	0.014
	2041–2070	0.002	−0.000	0.015	0.007	0.006	−0.007	0.011	0.012	−0.005
	2071–2100	0.006	0.004	−0.032	0.013	0.014	−0.013	0.019	0.028	−0.010

4. Conclusions and Future Work

This study assessed the present-day characteristics as well as the impact of future climate change on CWD, IR, and WA over West Africa. Ensembles of regional climate model simulations were used to derive these hydrological variables for current and future periods. A comparison of a historical period (1976–2005) with two future periods has been carried out, namely, the mid-future (2041–2070) and far future (2071–2100) under two emission scenarios.

Regional climate model simulation-derived CWD, IR, and WA are first validated in reproducing the present-day characteristics. The results indicate that the ensemble mean of the model-derived outputs reproduced the prevailing spatial pattern of crop water demand and irrigation requirement. Moreover, the water surplus part of the domain was correctly delineated, particularly in the Guinea Coast, from the water deficit regions of north of latitude 10°N, despite having biases. The ensemble model also simulated the annual cycle of water supply and the bimodal pattern of the CWD and IR curves correctly.

Projections show that CWD and IR are expected to increase in future warmer climates. Regions that are expected to experience the largest projected increment in CWD and IR lies mostly within the Sahel. The strongest increment is noted for the end of the 21st century and when the RCP8.5 scenario is followed. CWD is projected to increase by 0.75–1.05 mm/day over Savannah and Sahel by the end of the century. IR is also projected to increase by 1–1.4 mm/day towards the end of the century in the Sahel and parts of Savannah.

Future WA, on the other hand, is projected to decline, particularly for the end of the century and when the RCP8.5 scenario is followed. For the RCP4.5 scenario, a slight increment in WA is also noted over parts of Guinea, Sierra Leone, Liberia, southern Côte d’Ivoire and southern Ghana. The decline in WA is particularly higher over south-eastern parts of Guinea Coast. The largest decline in WA is noted over Guinea and most of the eastern parts of West Africa by up to 0.5–0.7 mm/day at the end of the century for the RCP 8.5 scenario.

By a comparison of present-day water resource potential per capita, particularly that of groundwater resources, the region has more resources compared to Europe and Asia [37]. However, the current utilization of both surface and groundwater resources for irrigated agriculture in the target region is much smaller than any other region in the developing world. Given these two competing factors (current underutilization of potential resources and future threat), cautious expansion of irrigation and cultivation of less water-demanding crops are recommended adaptation strategies to improve near-term food security and reduce future crop failure frequency. Technological adaptation, such as improvements in irrigation efficiency, is also another strategy that could partly alleviate some of the problems. If indeed technologically possible, this adaptation could effectively mitigate many adverse effects of climate change impacts by reducing groundwater pumping, irrigation water demand, and decreasing the need for land retirement due to excessive soil salinization [38].

Future work could consider a number of details to explore the sensitivity of key agro-meteorological and hydrological estimates computed in this assessment. For instance, effective precipitation can be computed differently, which potentially yields a different estimation of IR, and, therefore, future studies should explore various ways of its estimates

to quantify the uncertainty associated with it. The crop coefficient (K_c) value used in the computation of crop water demand also assumes values close to unity, which represents the values for the main crops cultivated in the region. Future assessments targeting different kinds of crops with smaller values of K_c need to consider changing the values of crop water demand and the corresponding IR. From the WA side, there is also uncertainty in future water supply under climate change, due to large variation in projected precipitation among climate models. It has to be noted that IR and WA projections for planning purposes depend on changes in population growth and changes in agricultural land use; therefore, future studies should consider these factors as well.

Supplementary Materials: The following supporting information can be downloaded at: <https://www.mdpi.com/article/10.3390/atmos13071155/s1>, Figure S1: Spatial correlation between CWD (mm/day) derived from Hargreaves (HETo) and Baier-Robertson (BRETo), Figure S2: Spatial difference between modelled and observed CWD (mm/day) for (a) HETo and (b) BRETo, Figure S3: Projected changes in crop water demand (mm/day) computed using Hargreaves (top panel) and Baier-Robertson (bottom panel) methods for mid-future (left column) and far future (right column) from the ensemble mean of regional climate models driven under RCP 4.5, Figure S4: Projected changes in irrigation demand (mm/day) computed using Hargreaves (top panel) and Baier-Robertson (bottom panel) methods for mid-future (left column) and far future (right column) from the ensemble mean of regional climate models driven under RCP 4.5, Figure S5: Projected changes in water availability (mm/day) for mid-future (left column) and far future (right column) from the ensemble mean of regional climate models driven under RCP 4.5.

Author Contributions: Conceptualization, I.E.G., G.T.D., J.D.I. and J.D.; methodology, I.E.G. and G.T.D.; software, I.E.G. and G.T.D.; validation, I.E.G.; formal analysis, I.E.G. and G.T.D.; resources, I.E.G., G.T.D., J.D.I. and J.D.; data curation, I.E.G.; writing—original draft preparation, I.E.G. and G.T.D.; writing—review and editing, I.E.G., G.T.D., J.D.I. and J.D.; visualization, I.E.G. and G.T.D.; supervision, G.T.D., J.D.I. and J.D.; project administration, I.E.G. and G.T.D.; funding acquisition, J.D. All authors have read and agreed to the published version of the manuscript.

Funding: This research received no external funding.

Institutional Review Board Statement: Not applicable.

Informed Consent Statement: Not applicable.

Data Availability Statement: The CHIRPS and ERA5 datasets were derived from climate explorer website (<https://climexp.knmi.nl/start.cgi> accessed on 7 June 2022) while the regional climate models were retrieved from the Earth System Grid Federation (ESGF) portal (<https://esgf-data.dkrz.de/projects/esgf-dkrz/> accessed on 7 June 2022).

Acknowledgments: The authors would like to thank the two anonymous reviewers for their constructive comments and useful suggestions. Also, thanks to the editorial and support team of this journal for their efforts during the review stage.

Conflicts of Interest: The authors declare no conflict of interest.

References

1. World Bank Group. Agriculture Development in West Africa: Improving Productivity through Research and Extension. *World Bank Group*. Available online: <https://www.worldbank.org/en/results/2013/03/28/agriculture-development-in-west-africa-improving-productivity-through-research-and-extension> (accessed on 30 August 2016).
2. Goedde, L.; Ooko-Ombaka, A.; Pais, G. Winning in Africa's Agricultural Market. McKinsey & Company. Available online: <https://www.mckinsey.com/industries/agriculture/our-insights/winning-in-africas-agricultural-market#> (accessed on 8 June 2022).
3. United States Geological Survey. West Africa: Land Use and Land Cover Dynamics. Available online: <https://eros.usgs.gov/westafrica/population> (accessed on 30 April 2022).
4. Nikolaou, G.; Neocleous, D.; Christou, A.; Kitta, E.; Katsoulas, N. Implementing sustainable irrigation in water-scarce regions under the impact of climate change. *Agronomy* **2020**, *10*, 1120. [CrossRef]
5. Döll, P. Impact of climate change and variability on irrigation requirements: A global perspective. *Clim. Chang.* **2020**, *54*, 269–293. [CrossRef]

6. Elgaali, E.; Garcia, L.A.; Ojima, D.S. High resolution modeling of the regional impacts of climate change on irrigation water demand. *Clim. Chang.* **2009**, *84*, 441–461. [[CrossRef](#)]
7. Fischer, G.; Tubiello, F.N.; Velthuis, H.; Wiberg, D.A. Climate change impacts on irrigation water requirements: Effects of mitigation, 1990–2080. *Technol. Forecast. Soc. Chang.* **2007**, *74*, 1083–1107. [[CrossRef](#)]
8. Konzmann, M.; Gerten, D.; Heinke, J. Climate impacts on global irrigation requirements under 19 GCMs, simulated with a vegetation and hydrology model. *Hydrol. Sci. J.* **2013**, *58*, 88–105. [[CrossRef](#)]
9. Rodríguez, J.A.; Weatherhead, E.K.; Knox, J.W.; Camacho, E. Climate change impacts on irrigation water requirements in the Guadalquivir river basin in Spain. *Reg. Environ. Chang.* **2007**, *7*, 149–159. [[CrossRef](#)]
10. Sylla, M.B.; Pal, J.S.; Faye, A.; Dimobe, K.; Kunstmann, H. Climate change to severely impact West African basin scale irrigation in 2 °C and 1.5 °C global warming scenarios. *Sci. Rep.* **2018**, *8*, 14395. [[CrossRef](#)]
11. Li, J.; Fei, L.; Li, S.; Xue, C.; Shi, Z.; Hinkelmann, R. Development of “water-suitable” agriculture based on a statistical analysis of factors affecting irrigation water demand. *Sci. Total. Environ.* **2020**, *744*, 140986. [[CrossRef](#)]
12. Giorgi, F.; Jones, C.; Asrar, G.R. Addressing climate information needs at the regional level: The CORDEX framework. *World Meteorol. Organ. Bull.* **2009**, *58*, 175.
13. Funk, C.; Peterson, P.; Landsfeld, M.; Pedreros, D.; Verdin, J.; Shukla, S.; Husak, G.; Rowland, J.; Harrison, L.; Hoell, A. The climate hazards infrared precipitation with stations—a new environmental record for monitoring extremes. *Sci. Data* **2015**, *2*, 150066. [[CrossRef](#)]
14. Hersbach, H.; Bell, B.; Berrisford, P.; Dahlgren, P.; Horányi, A.; Muñoz, J.; Nicolas, J.; Radu, R.; Schepers, D.; Simmons, A.; et al. The ERA5 Global Reanalysis: Achieving a detailed record of the climate and weather for the past 70 years. In Proceedings of the 22nd EGU General Assembly, online, 4–8 May 2020; p. 10375. [[CrossRef](#)]
15. Earth System Grid Federation (ESGF) portal. Available online: <https://esgf-data.dkrz.de/projects/esgf-dkrz/> (accessed on 1 June 2020).
16. Samuelsson, P.; Gollvik, S.; Kupiainen, M.; Kourzeneva, E.; Berg, W.J. The surface processes of the Rossby Centre regional atmospheric climate model (RCA4). SMHI. 2015. Available online: <https://www.diva-portal.org/smash/record.jsf?pid=diva2:948138> (accessed on 7 June 2022).
17. Rockel, B.; Will, A.; Hense, A. The regional climate model COSMO-CLM (CCLM). *Meteorol. Z.* **2008**, *17*, 347–348. [[CrossRef](#)]
18. Jacob, D.; Van, B.J.J.M.; Andrae, U.; Elgered, G.; Fortelius, C.; Graham, L.P.; Jackson, S.D.; Karstens, U.; Köpken, C.; Lindau, R.; et al. A comprehensive model inter-comparison study investigating the water budget during the BALTEX-PIDCAP period. *Meteorol. Atmos. Phys.* **2001**, *77*, 19–43. [[CrossRef](#)]
19. Giorgetta, M.A.; Jungclaus, J.; Reick, C.H.; Legutke, S.; Bader, J.; Böttinger, M.; Brovkin, V.; Crueger, T.; Esch, M.; Fieg, K. Climate and carbon cycle changes from 1850 to 2100 in MPI-ESM simulations for the Coupled Model Intercomparison Project phase 5. *J. Adv. Model. Earth Syst.* **2013**, *5*, 572–597. [[CrossRef](#)]
20. Vuuren, D.P.; Edmonds, J.; Kainuma, M.; Riahi, K.; Thomson, A.; Hibbard, K.; Hurtt, G.C.; Kram, T.; Krey, V.; Lamarque, J.F.; et al. The representative concentration pathways: An overview. *Clim. Chang.* **2011**, *109*, 5. [[CrossRef](#)]
21. Baier, W.; Robertson, G.W. Estimation of latent evaporation from simple weather observations. *Can. J. Plant. Sci.* **1965**, *45*, 276–284. [[CrossRef](#)]
22. Hargreaves, G.H.; Samani, Z.A. Reference crop evapotranspiration from temperature. *Appl. Eng. Agric.* **1985**, *1*, 96–99. [[CrossRef](#)]
23. Food and Agriculture Organization of the United Nations. Crop Evapotranspiration-Guidelines for Computing Crop Water Requirements-FAO Irrigation and Drainage Paper 56. 1998. Available online: <https://www.fao.org/3/x0490e/x0490e00.htm#Contents>. (accessed on 1 June 2020).
24. Brouwer, C.; Heibloem, Y. *Irrigation Water Needs [Irrigation Water Management Training Manual No. 3]*; Food and Agriculture Organization of the United Nations: Rome, Italy, 1986.
25. World Meteorological Organization. Guide to Climatological Practices. *Secretariat of the World Meteorological Organization*. 2018. Available online: https://library.wmo.int/doc_num.php?explnum_id=5541 (accessed on 1 April 2022).
26. Mann, H.B. Nonparametric tests against trend. *Econometrica* **1945**, *13*, 245–259. [[CrossRef](#)]
27. Gilbert, R.O. *Statistical Methods for Environmental Pollution Monitoring*; Van Nostrand Reinhold Company: New York, NY, USA, 1987.
28. Sirois, A.; Annex, E. A brief and biased overview of time-series analysis of how to find that evasive trend. In *WMO/EMEP Workshop on Advanced Statistical Methods and their Application to Air Quality Data Sets, (Helsinki, 14–18 September 1998)*; Global Atmosphere Watch No. 133, WMO TD-No. 956; World Meteorological Organization: Geneva, Switzerland, 1998. Available online: https://library.wmo.int/doc_num.php?explnum_id=10098 (accessed on 7 June 2022).
29. Iloeje, N.P. *A New Geography of Nigeria*; Williams Colwes Ltd.: Longman, UK, 1981.
30. Omotosho, J.B.; Abiodun, B.J. A numerical study of moisture build-up and rainfall over West Africa. *Meteorol. Appl.* **2007**, *14*, 209–225. [[CrossRef](#)]
31. Abiodun, B.J.; Salami, A.T.; Matthew, O.J.; Odedokun, S. Potential impacts of afforestation on climate change and extreme events in Nigeria. *Clim. Dyn.* **2013**, *41*, 277–293. [[CrossRef](#)]
32. Gbode, I.E.; Ogunjobi, K.O.; Dudhia, J.; Ajayi, V.O. Simulation of wet and dry West African monsoon rainfall seasons using the Weather Research and Forecasting model. *Theor. Appl. Climatol.* **2019**, *138*, 1679–1694. [[CrossRef](#)]

33. Joyce, B.; Vicuña, S.; Dale, L.; Dracup, J.; Hanemann, M.; Purkey, D.; Yates, D. Climate Change Impacts on Water for Agriculture in California: A Case Study in the Sacramento Valley. Document de Travail, California Climate Change Center, White Paper. Available online: <http://citeseerx.ist.psu.edu/viewdoc/download?doi=10.1.1.386.3114&rep=rep1&type=pdf> (accessed on 30 April 2022).
34. Hawkins, E.; Sutton, R. The Potential to Narrow Uncertainty in Regional Climate Predictions. *Bull. Am. Meteorol. Soc.* **2009**, *90*, 195–1108. [[CrossRef](#)]
35. Druyan, L.M. Studies of 21st-century precipitation trends over West Africa. *Int. J. Clim.* **2011**, *31*, 1415–1424. [[CrossRef](#)]
36. Sylla, M.B.; Nikiema, P.M.; Gibba, P.; Kebe, I.; Klutse, N.A.B. Climate Change over West Africa: Recent Trends and Future Projections. In *Adaptation to Climate Change and Variability in Rural West Africa*; Yaro, J.A., Hesselberg, J., Eds.; Springer International Publishing: Berlin/Heidelberg, Germany, 2016; pp. 25–40.
37. Food and Agriculture Organization of the United Nations. Review of World Water Resources by Country. Food and Agriculture Organization of the United Nations. 2003. Available online: <https://www.fao.org/3/Y4473E/y4473e.pdf> (accessed on 30 April 2022).
38. Hopmans, J.W.; Maurer, E. Impact of Climate Change on Irrigation Water Availability, Crop. Water Requirements and Soil Salinity in the San Joaquin Valley; University of California Water Resources Center: Riverside, CA, USA. Available online: <http://ciwr.ucanr.edu/files/169880.pdf> (accessed on 30 April 2022).